A Study on the Usefulness of an Ankle Joint Examination Assistive Device using a 3D Printing

Dong-Hee Hong[1], Eun-hye Kim[2], Young-Cheol Joo[3,*]

[1]Department of Radiological Science, Shinhan University
[2]Health Science Research Center, Korea University, Seoul, Republic of Korea
[3]Department of Radiology, Samsung Medical Center, Seoul, Republic of Korea

Received: November 28, 2023. Revised: December 27, 2023. Accepted: December 31, 2023.

ABSTRACT

The mortise view radiography procedure is an ankle joint examination and observes the presence of trauma, sprain, or dislocation suspected in the ankle joint. The auxiliary equipment used during the mortise view radiography procedure can generate artifacts in the radiograph images and is not diverse enough to be custom-made for each patient; not cost-efficient. The purpose of this study is to create a custom assistive device to support mortise view radiography procedure. This study utilized 3D printing technology to create the mortise view radiography procedure assistive device (ShinHan Device; SHD). The lengths of the tibiotalar joint (TTJ), talar calcaneal joint (TCJ), and medial joint (MJ) were measured and evaluated by five researchers using both SHD and the prototype Hologic tool. The mean ranges were found to be 39.42-39.47 mm for TTJ, 31.41-31.57 mm for TCJ, and 21.21-21.23 mm for MJ while using SHD device. On the other hand, the measurements showed mean ranges of 39.73-39.79 mm for TTJ, 31.46-31.50 mm for TCJ, and 21.31-21.35 mm for MJ while using the Hologic tool. Based on this study results, the error ranges at all positions decreased by 24% for TTJ, 17% for TCJ, and 36% for MJ when using SHD device compared to the Hologic tool. Moreover, when SHD was used, it allowed for a highly reproducible examination posture (ICC = 0.99), and it enabled the acquisition of radiograph images without artifacts, which were present in the Hologic tool.

Keywords: 3D Printer, Ankle joint, Mortise view, Assistive device, General radiograph

I. INTRODUCTION

The ankle joint supports the body and provides propulsion, and it is composed of ligaments that connect 9 bones. The most common pathology that occurs in the ankle joint is a sprain, which happens in nearly half of the cases during physical activity[1-3]. Ankle joint sprains are not only the most frequent musculoskeletal injuries but also often leave residual symptoms, such as recurrent sprains in around 40% of patients after treatment[4-6]. Calcaneal fractures account for 1-2% of all fractures[7-9]. These fractures occur due to high loads and can lead to severe and permanent functional impairment of the ankle[10-12]. Therefore, accurately identifying the location of the initial pathology and providing appropriate treatment and care the crucial.

For early diagnosis and proper treatment of ankle joint issues, ankle joint radiographic procedures are essential. The examination methods include the ankle joint anteroposterior (AP) projection, ankle joint mediolateral projection, ankle joint oblique projection,

* Corresponding Author: Young-Cheol Joo E-mail: hansound2@hanmail.net Tel: +82-31-870-3415
Address: 95 Hoam-ro, Uijeongbu, Geonggi 11644 Republic of Korea

ankle mortise view, ankle joint AP stress projection, and subtalar joint AP axial oblique projection[13-17]. The mortise view is a diagnostic method used to assess fragment location and graft evaluation after surgery, evaluate fracture treatment, assess chondral injuries, and evaluate ankle osteoarthritis[18-20]. During the procedure, the radiologic technologist positions the dorsum of the foot of the side being examined perpendicular to the ground and rotates it inward by 15° to 20°[21-23]. The mortise view allows visualization of the talocrural joint, mortise joint, and talofibular joint without overlap.

Generally, ankle joint fractures are detectable in radiographic procedures, but microfractures might be overlooked[24]. Detecting such microfractures is crucial, so maintaining a consistent position during ankle joint radiography is important. However, due to the diversity of ankle joint forms among patients and the difficulty in consistently implementing the same position during the radiography procedures, obtaining the textbook-required radiography images from all patients can be practically challenging. To address these issues, the development of examination aassistive devices is essential to maintain a consistent patient position during the mortise view radiography procedure[9,25-27].

In this study, we evaluated the clinical utility of a 3D-printed ankle joint examination assistive device to achieve a consistent ankle joint rotation ankle and examiner posture, as well as standardized image depiction during the mortise view examination.

II. MATERIALS AND METHODS

1. Experimental Equipment and Phantom

In this study, the radiographic imaging equipment (Innovision DXII, DK medical system, Republic of Korea), and the foot phantom used was the RSD Anthropomorphic food ankle phantom RS-116T (Universal medical, CA, United States). Two types of auxiliary assistive devices were used: a self-made assistive device using a 3D printer by the researchers (ShinHan Device; SHD) (Fig 1-(b)) and the existing prototype called hip positioning fixture for Hologic bone densitometer hip positioning fixture 010-0141 (Hologic, MA, United States) (Fig. 1-(a)).

(A) Hip Positioning Fixture for Hologic (Hologic tool)

(B) ShinHan Device (SHD)

Fig. 1. The assistive devices used in this study.

2. Manufacturing Assistive Device

The design for 3D printing was created using the CAD program Tinkercad (Autodesk, CA, United States). The 3D printing output was produced using a 3D printer Form 2 (Formlabs, MA, United States) with stereolithography apparatus (SLA) technology, and the material used was clear resin. After printing, the assistive devices were washed using form wash and cured using form cure (Fig 2).

The SHD consists of five parts, each with its specific role (Fig 3). First, angle adjustment parts; these parts have an angle adjustment function that allows the auxiliary assistive device to be tilted according to the angle of the ankle (Fig 3-(a)). Second, the support base; this part provides stability and prevents the angle adjustment part from shaking

(Fig 3-(b)).

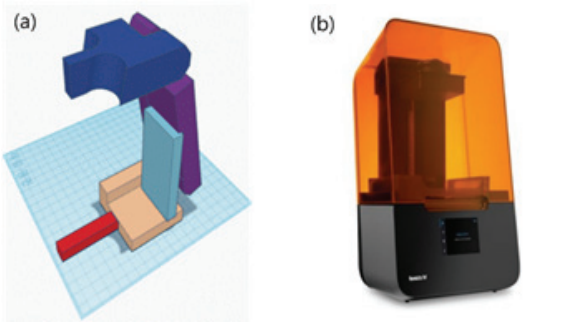

(A) 3D modeling using CAD program (B) SLA type 3D printer

Fig. 2. SHD Fabrication Process.

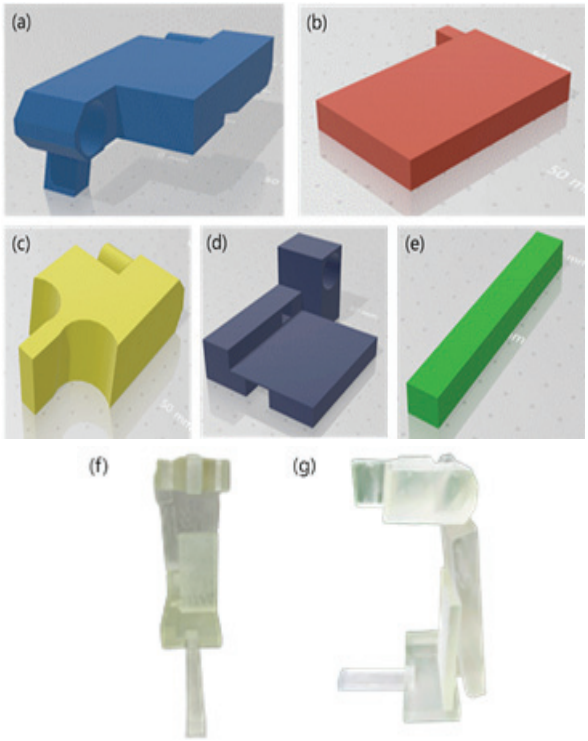

Fig. 3. SHD components.
(a) angular adjusting part, (b) supporting part for angular adjusting part, (c) foot supporting part, (d) base part of the entire component, (e) heel length controller, (f) combined SHD frontal view, (g) combined SHD lateral view

Third, foot support, this part directly supports the foot (Fig 3-(c)). Fourth, SHD bottom; this part forms the base of the entire assistive device and provides support by connecting with the angle adjustment, support base and position adjustment part (Fig 3-(d)). Fifth, position adjustment; this part adjusts the position of the heel during the examination (Fig 3-(e)). Finally, SHD; the complete assembly of all parts forming the assistive device (Fig 3-(f), (g)).

For the mortise view radiograph procedure, the foot is tilted at an angle of 15° to 20°. The assistive device supports the foot at the appropriate angle, allowing control of foot movement and maintaining a consistent ankle joint inclination angle during the examination.

3. Image acquisition & measurement method

The method of acquiring images involved placing the phantom in the image receptor in the mortise view examination position and entering vertically toward the center of both lateral and medial malleoli. The radiographic examination conditions were set at 60 kV, 100 mA, and 63 ms. The source to image distance (SID) was set at 100 cm, and the field of view (FOV) (Fig. 4).

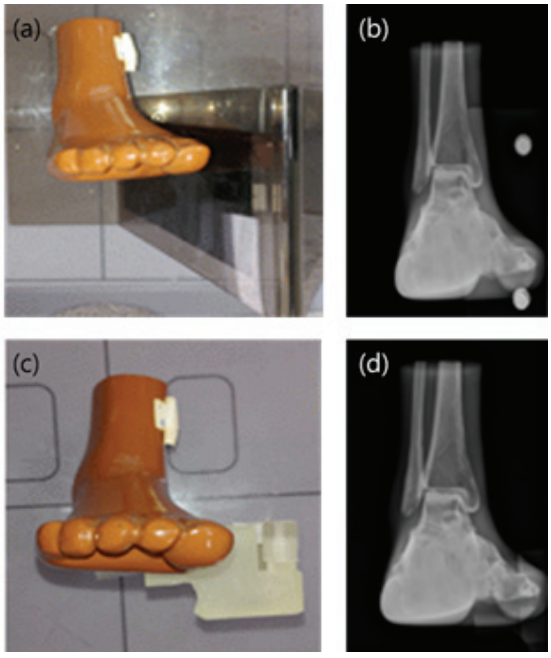

Fig. 4. Radiograph image comparison between hologictool and SHD.
(a) mortise view with the hologic tool, (b) radiograph image of mortise view with the hologic tool, (c) mortise view with the SHD, (d) radiograph image of mortise view with the SHD

In this study, image measurements were conducted by five operators from the Radiology Department at Shinhan University who participated in the study. They performed 10 measurements each at different times over a span of 10 days. Images acquired using the SHD method totaled 1,500 radiographic images, with 300 images per operator, while images obtained using the Hologic tool method also amounted to the same number. The measured area included the tibiofibular joint, the mortise joint, and the talar neck joint with the following measurement methods (figure 5). Talotibial joint (TTJ) is the length between the inner malleolus end and a virtual parallel line connecting the tibial and fibular bones. Talocrural joint (TCJ) is the length between the lateral malleolus and the talar neck on the same parallel line as TTJ. Mortise joint (MJ) is the length between a virtual vertical line at the midpoint between the tibial and fibular bones and the talar bone.

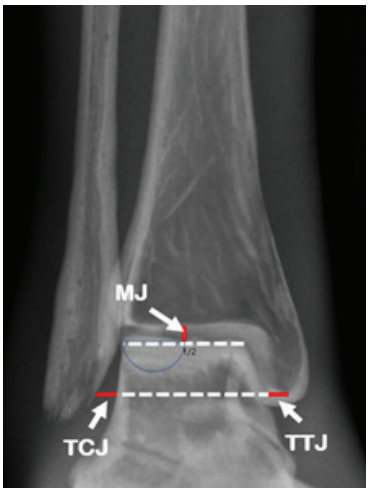

Fig. 5. Radiograph Image Measurement method.

4. Data evaluation method

For radiographic image evaluation in this study, medical image standard (digital imaging and communications in medicine; DICOM) files were assessed using ImageJ software (National Institutes of Health, MD, United States). Statistical analysis was performed using the SPSS software (SPSS version 26, IL, United States). The data evaluation approach of this study involved five assessors presenting descriptive statistics (mean, standard deviation, minimum, maximum values) for the measurements taken at each location from the 3,000 images acquired using the SHD and Hologic tool methods. Furthermore, the interrater reliability (intraclass correction; ICC) among the operators for the measurements was analyzed. Independent sample t-tests were conducted to compare the mean measurements for each measurement location between the two tools in each image.

III. RESULTS

The results of the measurements of TTJ, TCJ, and MJ lengths according to the measurement methods are as follows. When using SHD tool, the length of TTJ ranged from 39.42 to 39.47 mm, the length of TCJ ranged from 31.41 to 31.57 mm, and the length of MJ ranged from 21.21 to 21.23 mm. When using the Hologic tool, the length of TTJ ranged from 39.73 to 39.79 mm, the length of TCJ ranged from 31.46 to 31.50 mm, and the length of MJ ranged from 21.31 to 21.35 mm. The inter-rater reliability for each measurement was all 0.99 (Table 1, 2, 3).

The results of the mean comparison of TTJ, TCJ, and MJ lengths measured with SHD and Hologic tool are as follows. For TTJ, the measurements were 39.43±1.20 mm with SHD and 39.76±1.49 mm with Hologic tool. For TCJ, the measurements were 31.50±0.96 mm with SHD and 31.48±1.13 mm with Hologic tool. For MJ, the measurements were 21.22±0.82 mm with SHD and 21.33±1.12 mm with Hologic tool. Additionally, the mean differences between the two groups for TTJ and MJ were statistically significant ($p<0.01$, $p<0.02$), but for TCJ, there was no statistically significant difference ($p>0.61$) (Table 4). The difference in mean values between the TTJ and MJ groups was statistically significant ($p<0.01$, $p<0.02$), but not statistically significant in the TCJ group ($p>0.61$) (Table 4).

Table 1. Descriptive statistics and reliability analysis result by operators according to the measurement method in TTJ

Location of measurement	Variables	Operator	N	Mean ± SD (mm)	Min	Max	ICC
TTJ	SHD	A	300	39.45 ± 1.22	37.1	41.2	0.99
		B		39.42 ± 1.23	37.1	41.3	
		C		39.47 ± 1.18	37.2	41.4	
		D		39.38 ± 1.21	37.2	41.3	
		E		39.44 ± 1.16	37.3	41.2	
	Hologic tool	A	300	39.73 ± 1.48	37.1	42.4	0.99
		B		39.74 ± 1.48	37.2	42.5	
		C		39.78 ± 1.49	37.2	42.4	
		D		39.79 ± 1.51	37.3	42.3	
		E		39.74 ± 1.50	37.1	42.4	

1 TTJ is talotibial joint and SHD is a self-made assistive device by researchers.
2 A, B, C, D, and E are operators.
3 All measured values were expressed as mean±SD, ICC was intraclass correlation coefficient, and p-value of all ICC was p<0.01.

Table 2. Descriptive statistics and reliability analysis result by operators according to the measurement method in TCJ

Location of measurement	Variables	Operator	N	Mean ± SD (mm)	Min	Max	ICC
TCJ	SHD	A	300	31.41 ± 0.98	29.7	33.2	0.99
		B		31.44 ± 0.96	29.7	33.3	
		C		31.54 ± 0.95	29.8	33.2	
		D		31.55 ± 0.97	29.7	33.3	
		E		31.57 ± 0.96	29.7	33.3	
	Hologic tool	A	300	31.46 ± 1.17	29.1	33.9	0.99
		B		31.47 ± 1.16	29.2	33.8	
		C		31.50 ± 1.16	29.2	33.8	
		D		31.49 ± 1.09	29.1	33.7	
		E		31.48 ± 1.11	29.3	33.8	

1 TCJ is talotibial joint and SHD is a self-made assistive device by researchers.
2 A, B, C, D, and E are operators.
3 All measured values were expressed as mean±SD, ICC was intraclass correlation coefficient, and p-value of all ICC was p<0.01.

Table 3. Descriptive statistics and reliability analysis result by operators according to the measurement method in MJ

Location of measurement	Variables	Operator	N	Mean ± SD (mm)	Min	Max	ICC
MJ	SHD	A	300	21.21 ± 0.82	19.5	22.7	0.99
		B		21.22 ± 0.85	19.6	22.9	
		C		21.21 ± 0.80	19.5	22.7	
		D		21.23 ± 0.83	19.4	22.8	
		E		21.23 ± 0.81	19.6	22.8	
	Hologic tool	A	300	21.35 ± 1.14	19.1	23.8	0.99
		B		21.31 ± 1.12	19.2	23.7	
		C		21.35 ± 1.13	19.1	23.9	
		D		21.32 ± 1.14	19.3	23.8	
		E		21.32 ± 1.08	19.1	23.8	

1 MJ is talotibial joint and SHD is a self-made assistive device by researchers.
2 A, B, C, D, and E are operators.
3 All measured values were expressed as mean±SD, ICC was intraclass correlation coefficient, and p-value of all ICC was p<0.01.

Table 4. Mean comparison results of length of TTJ, TCJ, and MJ measured by SHD and Hologic tool

Location of measurement	Variables	N	Mean ± SD (mm)	Min	Max	t	p
TTJ	SHD	1500	39.43 ± 1.20	37.1	41.4	-6.50	0.01
	Hologic tool		39.76 ± 1.49	37.1	42.5		
TCJ	SHD		31.50 ± 0.96	29.7	33.3	0.50	0.61
	Hologic tool		31.48 ± 1.13	29.1	33.9		
MJ	SHD		21.22 ± 0.82	19.4	22.9	-3.05	0.02
	Hologic tool		21.33 ± 1.12	19.1	23.9		

1 TTJ: talotibial joint, TCJ: talocrural joint, MJ: mortise joint2 A, B, C, D, and E are operators.
2 The p value is calculated by the independent t-test

IV. DISCUSSION

The ankle joint performs weight-bearing, standing, and walking functions while requiring motility[28-29]. In this joint that performs these functions, sprains and fractures commonly occur[1-3,30]. Early treatment and accurate examination are essential to prevent residual symptoms when the ankle joint is damaged[30-31]. To conduct accurate examinations, the radiologic technologist's positioning must always be consistent, and standardized radiographic images must be obtained. Therefore, in this study, an ankle joint examination assistive device was developed. Using 3D printing technology, a rigid and cost-effective patient-customized assistive device was created[32-33]. This provisional 3D printing technology is useful in radiation therapy assistive devices, and various studies are underway [34]. In a preliminary study on assistive device production using a 3D printer, compensation for dual angles was made during the Law method using an assistive device[35]. In this case, the assistive device appeared in the radiographic image, causing artificial shading, which deteriorates image quality and makes it difficult to determine the lesion's location.

In another study, although 3D printing technology was not used, to avoid the occurrence of artifacts due to the use of assistive devices, a different approach was taken in the shape of the assistive device, and instead of larger and less practical assistive devices, separable and downsized assistive devices were created[19].

The study compared the changes in the lengths of TTJ, TCJ, and MJ when using SHD and Hologic tools based on the measuring operators. The results of the study showed that the ICC values for TTJ, TCJ, and MJ were all 0.99 when using SID and Hologic tools. Specifically, TCJ measurements showed that the mean value was 0.02 mm higher with SHD (31.50±0.96 mm) compared to Hologic tool (31.48±1.13 mm). However, this mean difference was not significant; SHD exhibited lower measurement errors. For TTJ measurements, SHD had a mean value of 39.43±1.20 mm, while Hologic tool had a mean value of 39.76±1.49 mm, resulting in a difference of 0.33 mm. For MJ measurements, SHD had a mean value of 21.22±0.82 mm, while Hologic tool had a mean value of 21.33±1.12 mm, resulting in a difference of 0.11 mm. Significant differences were observed in the mean differences for TTJ and MJ, with lower error ranges in the measurements.

This suggests that SHD was easier to use for the mortise view examination positioning, leading to these results. Therefore, this study utilized 3D printing technology to create assistive devices that can be customized for patients, making it easier to maintain their posture during examinations. However, one limitation of this study was that the angles were designed specifically for the mortise view

examination. To enhance the performance of the assistive device, it is important to have versatility in angles that can be used. Therefore, future research should focus on developing assistive devices that allow for flexible angle adjustments during ankle joint examinations, ensuring high reproducibility of images regardless of the radiologic technologist's proficiency.

V. CONCLUSION

In conclusion, this study evaluated the usefulness of an ankle joint radiographic examination assistive device produced using a 3D printer for consistent ankle joint rotation angles and standardized image depiction in the mortise view examination. The average differences in the measurements of joint spacing of TTJ, TCJ, and MJ were as follows when using the SHD tool: TTJ decreased by 0.85%, MJ decreased by 0.52%, and TCJ increased by 0.06%. There was no significant difference in reliability between using SHD and Hologic tool. However, the use of SHD resulted in a decrease in error ranges for TTJ by 24%, TCJ by 17%, and MJ by 36% compared to using the Hologic tool. Therefore, using SHD tool allowed for consistent patient positioning implementation similar to the Hologic tool, while achieving less error-prone image reproductions. Additionally, the use of the assistive device did not introduce artifacts into the images.

Reference

[1] P. A. Gribble, C. M. Bleakley, B. M. Caulfield, C. L. Docherty, F. Fourchet, D. T. P. Fong, J. Hertel, C. E. Hiller, T. W. Kaminski, P. O. McKeon, K. M. Refshauge, E. A. Verhagen, B. T. Vicenzino, E. A. Wikstrom, E. Delahunt, "Evidence review for the 2016 International Ankle Consortium consensus statement on the prevalence, impact and long-term consequences of lateral ankle sprains", British Journal of Sports Medicine, Vol. 50, No. 24, pp. 1496-1505, 2016. http://dx.doi.org/10.1136/bjsports-2016-096189

[2] B. R. Waterman, B. D. Owens, S. Davey, M. A. Zacchilli, P. J. Belmont, "The epidemiology of ankle sprains in the United States", The Journal of bone and joint surgery, Vol. 92, No. 13, pp. 2279-2284, 2010. http://dx.doi.org/10.2106/JBJS.I.01537

[3] F. Halabchi, M. Hassabi, "Acute ankle sprain in athletes: Clinical aspects and algorithmic approach", World journal of orthopedics, Vol. 11, No. 12, pp. 534-558, 2020. http://dx.doi.org/10.5312/wjo.v11.i12.534

[4] K. S. Sung, "Ankle sprains: epidemiology, anatomy and injury mechanism", Journal of the Korean Orthopaedic Association, Vol. 49, pp. 1-6. 2014. http://dx.doi.org/10.4055/jkoa.2014.49.1.1

[5] B. R. Waterman, B. D. Owens, S. Davey, M. A. Zacchilli, P. J. Belmont, "The Epidemiology of Ankle Sprains in the United States", The Journal of bone and joint surgery, Vol. 92, No. 13, pp. 2279-2284, 2010. http://dx.doi.org/10.2106/JBJS.I.01537

[6] J. R. Gurtowski, P. E. Levin, *Principles of orthopaedic practice*, New York: McGraw-Hill, pp. 1242-1260, 1989.

[7] M. Galluzzo, F. Greco, M. Pietragalla, A. D. Renzis, M. Carbone, M. Zappia, N. Maggialetti, A. D'andrea, G. Caracchini, V. Miele, "Calcaneal fractures: radiological and CT evaluation and classification systems", Acta Bio-Medica de l'Ateneo Parmense, Vol. 89, pp. 138-150, 2018. http://dx.doi.org/10.23750/ABM.V89I1-S.7017

[8] A. Daftary, A. H. Haims, M. R. Baumgaertner, "Fractures of the calcaneus: a review with emphasis on CT", Radiographics, Vol. 25, No. 5, pp. 1215-1226, 2005. http://dx.doi.org/10.1148/rg.255045713

[9] B. J. Sangeorzan, S. K. Benirschke, J. B. Carr, "Surgical management of fractures of the os calcis", Instructional Course Lectures, Vol. 44, pp. 359-370, 1995.

[10] L. A. Crosby, P. Kamins, "The history of the calcaneal fracture", Orthopaedic Review, Vol. 20, No. 6, pp. 501-509, 1991.

[11] C. Zhang, Z. M. Ye, P. Lin, X. D. Miao, "Lateral fracture-dislocation of the calcaneus: case reports and a systematic review", Orthopaedic Surgery, Vol. 13, No. 3, pp. 682-691, 2021.

http://dx.doi.org/10.1111/os.12913

[12] B. W. Long, F. Faeirs, J. H. Rollins, B. J. Smith, *Merrill's atlas of radiographic positioning and procedures,* 13th ed, St. Louis: Elsevier/Mosby, 2015.

[13] R. Lopez-Ben "Imaging of the subtalar joint", Foot and Ankle Clinics, Vol. 20, No. 2, pp. 223-241, 2015. http://dx.doi.org/10.1016/j.fcl.2015.02.009

[14] N. Krähenbühl, T. Horn-Lang, B. Hintermann, M. Knupp, "The subtalar joint: A complex mechanism", EFORT Open Rev, Vol. 2, No. 7, pp. 309-316, 2017. http://dx.doi.org/10.1302/2058-5241.2.160050

[15] D. T. Schwartz, *Emergency radiology: case studies*. 1st ed. New York: McGraw-Hill, 2017.

[16] E. D. Frank, N. A. Kravetz, D. E. O'Neill, T. H. Berquist, "Radiography of the ankle mortise", Radiologic technology, Vol. 62, No. 5, pp. 354-359, 1991.

[17] L. J. Prokuski, C. L. Saltzman, "Challenging fractures of the foot and ankle", Radiologic Clinics of North America, Vol. 35, No. 3, pp. 655-670, 1997. http://dx.doi.org/10.1016/S0033-8389(22)00598-X

[18] S. J. Seo, C. Y. Kim, J. H. Lee, H. D. Park, "The evaluation of usefulness of the newly manufactured immobilization device", The Journal of Korean Society for Radiation Therapy, Vol. 17, No. 1, pp. 45-55, 2005.

[19] C. C. M. A. Donken, M. H. J. Verhofstad, M. J. Edwards, M. C. Schoemaker, C. J. H. M. van Laarhoven, "Use of an acrylic mold for mortise view improvement in ankle fractures: a feasibility study", The Journal of Foot and Ankle Surgery, Vol. 50, No. 5, pp. 525-528, 2011. http://dx.doi.org/10.1053/j.jfas.2011.05.010

[20] M. Takao, M. Ochi, K. Naito, A. Iwata, Y. Uchio, K. Oae, T. Kono, K. Kawasaki, "Computed tomographic evaluation of the position of the leg for mortise radiographs", Foot & Ankle International, Vol. 22, No. 10, pp. 828-831, 2001. http://dx.doi.org/10.1177/107110070102201009

[21] K. George, M. William B, "Foot and ankle disorders: radiographic signs", Seminars In Roentgenology, Vol. 40, No. 4, pp. 358-379, 2005. http://dx.doi.org/10.1053/j.ro.2005.01.018

[22] A. A. Najefi, O. Buraimoh, J. Blackwell, A. Bing, R. Varrall, D. Townshend, A. Goldberg, "Should the tibiotalar angle be measured using an ap or mortise radiograph? Does it matter?", The Journal of Foot and Ankle Surgery, Vol. 58, No. 5, pp. 930-932, 2019. http://dx.doi.org/10.1053/j.jfas.2019.01.013

[23] P. V. Gourineni, A. E. Knuth, G. F. Nuber, "Radiographic evaluation of the position of implants in the medial malleolus in relation to the ankle joint space: anteroposterior compared with mortise radiographs", Journal of Bone and Joint Surgery, Vol. 81, No. 3, pp. 364-369, 1999. http://dx.doi.org/10.2106/00004623-199903000-00008

[24] E. C. R. Merchan, "Subtalar dislocations: long-term follow-up of 39 cases", Injury, Vol. 23, No. 2, pp. 97-100, 1992. http://dx.doi.org/10.1016/0020-1383(92)90041-p

[25] G. D. Kim, Y. T. Oh, "A benchmark study on rapid prototyping processes and machines: Quantitative comparisons of mechanical properties, accuracy, roughness, speed, and material cost", Journal of Engineering Manufacture, Vol. 222, No. 2, pp. 201-215, 2008. http://dx.doi.org/10.1243/09544054JEM724

[26] S. B. Choi, "Development of application indicators for the fabrication of radiotherapy auxiliary devices using 3D printing technology", The Graduate School of Bio-Medical Science, Master Thesis, Korea University, Republic of Korea, 2015.

[27] M. S. Yoon, S. M. Hong, Y. C. Heo, D. K. Han, "A Study on the Fabrication and Comparison of the Phantom for Computed Tomography Image Quality Measurements Using Three-Dimensions Printing Technology", Journal of Radiological Science and Technology, Vol. 41, No. 6, pp. 595-602, 2018. https://doi.org/10.17946/JRST.2018.41.6.595

[28] S. E. Munteanu, A. B. Strawhorn, K. B. Landorf, A. R. Bird, G. S. Murley, "A weightbearing technique for the measurement of ankle joint dorsiflexion with the knee extended is reliable", Journal of Science and Medicine in Sport, Vol. 12, No. 1, pp. 54-59, 2009. http://dx.doi.org/10.1016/j.jsams.2007.06.009

[29] J. Rose, J. G. Gamble, *Human Walking*. 3rded.

Philadelphia: Lippincott Williams and Wilkins, 2006.

[30] H. W. Lee, M. S. Oh, S. G. Han, J. T. Hopkins, "Unexpected inversion perturbation during a single-leg landing in patients with chronic ankle instability", Sports Biomechanics, pp. 1-15, 2023. http://dx.doi.org/10.1080/14763141.2023.2226649

[31] J. M. Meyer, J. Garcia, P. Hoffmeyer, D. Fritschy, "The Subtalar sprain: a roentgenographic study", Clinical Orthopaedics and Related Research, Vol. 226, pp. 169-173, 1988. http://dx.doi.org/10.1097/00003086-198801000-00023

[32] W. J. Choi, S. Y. Ye, D. H. Kim, "Making Aids of Magnetic Resonacnce Image Susing 3D Printing Technology", Journal of the Korean Society of Radiology, Vol. 10, No. 6, pp. 403-409, 2016. http://dx.doi.org/10.7742/jksr.2016.10.6.403

[33] W. J. Choi, D. H. Kim, "Making Human Phantom for X-ray Practice with 3D Printing", Journal of the Korean Society of Radiology, Vol. 11, No. 5, pp. 371-377, 2017. http://dx.doi.org/10.7742/jksr.2017.11.5.371

[34] T. Letcher, M. Waytashek, "Material Property Testing of 3D-Printed Specimen in PLA on an Entry-Level 3D Printer", ASME 2014 International Mechanical Engineering Congress and Exposition, Vol. 14, No. 20, pp. 3-8, 2014. https://doi.org/10.1115/IMECE2014-39379

[35] S. H. Kim, "Study on 3D Printer Producing of Assistive Devices for Vertical Incidence of Law Method", Journal of radiological science and technology, Vol. 43, No. 6, pp. 489-494, 2020.

3D 프린터를 이용한 발목관절 검사 보조기구의 유용성 연구

홍동희[1], 김은혜[2], 주영철[3,*]

[1]신한대학교 방사선학과
[2]고려대학교 보건안전융합과학과
[3]삼성의료원 영상의학과

요 약

Mortise view 검사는 발목관절 검사로써 발목관절의 외상이나 염좌, 탈구가 의심되는 병변의 유무를 관찰한다. mortise view 검사 시 사용되는 보조기구는 영상에 인공물을 발생하거나, 종류가 다양하지 않아 환자 맞춤형으로 제작되지 않고 가격이 비싸다. 이에 본 연구는 3D 프린팅 기술을 이용하여 mortise view 검사 보조기구(ShinHan Device; SHD)를 제작하였다. SHD를 사용했을 때와 시제품인 hologic tool을 사용했을 때의 목말종아리관절, mortise 관절, 목말정강관절의 길이를 5명의 연구자가 측정하여 평가하였다. SHD를 사용했을 때 평균값의 범위는 TTJ에서 39.42~39.47 mm, TCJ 31.41~31.57 mm, MJ 21.21~21.23 mm의 범위로 나타났다. hologic tool를 사용했을 때는 TTJ 39.73~39.79 mm, TCJ 31.46~31.50 mm, MJ 21.31~21.35 mm의 범위로 측정되었다. 본 연구결과, 모든 위치에서의 오차범위가 hologic tool에 비해 SHD를 사용 때 TTJ는 24%, TCJ는 17%, MJ는 36% 감소하였으며, SHD를 사용하였을 때 재현성 높은 검사자세를 구현할 수 있었으며(ICC=0.99), hologic tool에서 발생하던 인공물을 제거한 영상을 획득할 수 있었다.

중심단어: 3D 프린터, 발목관절, Mortise 촬영, 보조기구, 방사선, 일반촬영

연구자 정보 이력

	성명	소속	직위
(제1저자)	홍동희	신한대학교 방사선학과	조교수
(공동저자)	김은혜	고려대학교 보건안전융합과학과	연구교수
(교신저자)	주영철	삼성서울병원 영상의학과	방사선사